Energy Storage Technology and Converter Topology for Primary Frequency Control in Thermal Power Plant

Martin VINS, Jaroslav DRAGOUN, Martin SIROVY

Research and Innovation Centre for Electrical Engineering,
Faculty of Electrical Engineering, University of West Bohemia,
Univerzitni 2795/26, 301 00 Pilsen, Czech Republic

mvins@fel.zcu.cz, dragounj@fel.zcu.cz, sirovy@fel.zcu.cz

DOI: 10.15598/aeee.v19i2.3945

Article history: Received Sep 23, 2020; Revised Apr 14, 2021; Accepted May 11, 2021; Published Jun 30, 2021.

Abstract. *Motivation and complex process of energy storage technology and converter topology design suitable for integration in thermal power plant systems to improve flexibility and primary frequency control is presented in the paper. The case study of typical thermal power plant is included and optimal power and capacity are determined. Next, there are discussed and compared perspective accumulation technologies. Most perspective state of the art battery-based technologies are further in detail evaluated including employed methodology. The next part is focused on suitable converter topology design. Employed converter control algorithms including simulation results are presented.*

Keywords

Accumulation, battery, CHB, converter topology, Energy Storage, LCL filter, Li-ion, NaS, primary frequency control, selection, sizing, thermal power plant, VRF.

1. Introduction

The increasing trend of integration of renewable energy sources to the electrical grid implies increasing demands and new challenges to grid stability and control.

The conventional electricity sources as coal-fired thermal power plants are pushed into the background. Nevertheless, there are opportunities how to upgrade the current power plants by integrating of Battery Energy Storage System (BESS) to reduce stress on conventional sources caused by fast power transients in the grid and improve the system flexibility. The combined layout improves primary frequency control parameters (e.g., activation speed) and also can improve other control capabilities of power plant. Additional benefits of the combined solution are the well-dimensioned connection to the grid as well as the availability of free space.

Many studies have shown the technological and economic benefits of the BESS integration to the distribution grid. For example, an impact of the BESS on Transmission grid operation in Portugal, which has a large quantity of variable renewable energy sources is shown in [1]. The impact of multiple BESS on the central Europe transmission grid is shown in [2]. And optimal sizing of BESS based on vanadium redox flow batteries with the cost-benefit optimization is shown in [3].

The use of the battery energy storage for primary frequency control is discussed in detail in [4] but there are not assumed Li-ion batteries nor integration to thermal power plant. The paper [5] describes the use of batteries for primary frequency control but without specifics of integration to the thermal power plant. In our research, we have focused at first on the review and selection of the most suitable energy storage technology for the application and review and design of the suitable topology of frequency converters. This complex part of the system dimensioning and design has been described in this paper. In the second step we have focused on the complex system design, i.e., on the as-

pects of BESS integration next to the turbomachinery and common operation performance – results of this research have been published in our further paper [6].

2. Methodology

The methodology follows the design of the BESS. It summarizes some well-known principles, but it is broadened by the practical experiences from the electrical energy generation and some uncommon solutions are proposed. For example, the application of multilevel converters.

First of all, there is a need for a BESS size – power and capacity determination. This has been done due to project cooperation with case study power plant operators as well as steam turbines manufacturer. BESS dimensioning method and considered assumptions are described in Sec. 3.

There was also made an extensive overview of accumulation technologies which are described and compared in Sec. 4. Due to the default technology requirements, there are selected batteries (electrochemical accumulation). A method and a tool were made for comparison of the most industrially available (technologically ready) technologies of batteries from which the optimal technology of batteries is selected, described in Sec. 5.

In Sec. 6. , the choice of the BESS connection to the grid and converter topology is discussed. This is from the point of influence on the grid and the efficiency of the system. Also, the possible output power regulation is proposed and verified through the simulation results.

3. BESS Dimensioning

First, there is important to determine the optimal power of the energy storage. In Fig. 1, there is the power histogram used for primary frequency control based on 3 years period (2015–2018) from a 4×200 MW Czech coal-fired power plant. The maximum power used for the primary frequency control is 10 MW (5 % of nominal power), the reasonable power of the energy storage has been designed to 4 MW for covering $\sim$ 98 % of primary frequency control activation cases, as shown in Fig. 1. The primary frequency control usage is relatively equal in all four units (A, B, C, and D) of the power plant.

Capacity of the energy storage is determined by the steam turbine response and regulation times. It is assumed, that the energy storage covers the first moments of primary frequency control activation until the turbine changes its power. Heated turbine can fulfill

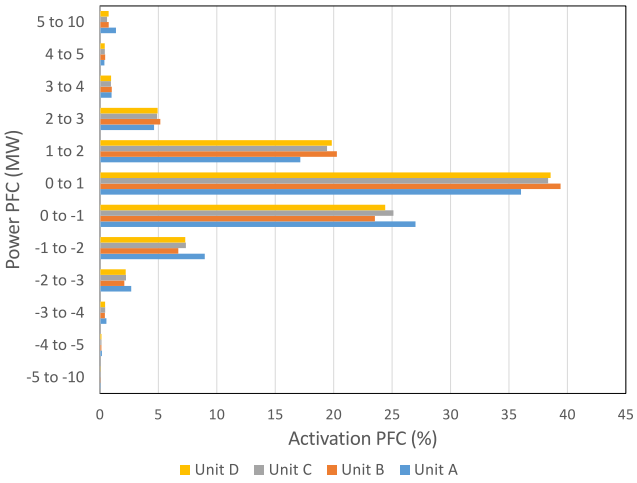

Fig. 1: Histogram of primary frequency control activation.

any power demand step within approximately 15 min without the negative effects of turbine lifetime. Based on this presumption, the optimal capacity has been determined to 1 MWh (taking 4 MW up to 15 min). This capacity has been estimated based on the control capabilities of general steam turbine and it takes into account the worst possible scenario of the turbine response time (regulation from any power). The capacity design can be further optimized for a specific application based on the specific capabilities of the target steam turbine and stability of the target electrical grid.

4. Accumulation Technology

For the optimal accumulation technology determination, the following main system requirements were formulated:

- fast response time,
- possibility of fast increase of power,
- fast transient from charging to discharging,
- low losses in charged state,
- low losses due to charging and discharging,
- accurate sizing,
- long lifetime,
- low costs.

A wide specter of accumulation technologies based on electro-thermal, electro-chemical and electro mechanical principles was considered. A simplified comparison can be seen in Tab. 1 [7].

There can be seen critical pros and cons of the compared technologies. Flywheels have a high efficiency

Tab. 1: Accumulation technology comparison [7].

Technology / Parameter	Flywheel	Battery	Thermal energy storage	Compressed air energy storage
Response time	seconds	miliseconds	minutes–hours	seconds–minutes
Lifetime	20+ years	0.5–20 years	10–30 years	20–40 years
Cycle efficiency	90–95 %	60–97 %	55–80 %	∼ 70 %
Daily selfdischarge	up to 20 % per hour	0.1–0.3 %	0.5–1 %	almost zero
Suitable storage duration	seconds–minutes	minutes–months	minutes–months	hours–months
Commercialization level	early	early / in progress	early	early / in progress

of the cycle but also a very high self-discharge which is not suitable for longer storing of the energy. On the contrary, the thermal energy storages have a low self-discharge but also a very slow response time which is not applicable for fast primary frequency control response. Compressed air energy storages are somewhere between the previous ones. Neither slow nor fast response time, neither low nor high cycle efficiency, and unnecessarily long energy-storing time. The most suitable accumulation technology for the assumed application was therefore selected electrochemical batteries. They have very fast response time and cycle efficiency, sufficient lifetime, and self-discharge. Specific battery technology selection is described in the next section.

5. Battery Technology

There were considered three battery technologies due to their high TRL and possible industrial applicability. They are Lithium-ion (Li-ion; specifically, $LiFePO_4$), Sodium-sulfur (NaS) and Vanadium Redox Flow (VRF) batteries [8].

There is important information to be stated, that the energy storage system can be realized via all the three technologies but only one is optimal from the technical-economical point of view. The economical evaluation criterion has been calculated as the future cost of investment based on Eq. (1) [8].

$$C_f = C_i \cdot r(i, L) + \sum_{j=1}^{j=L} C_o \cdot r(i, j), \tag{1}$$

where C_f (USD) are future costs which take into account investment C_i (USD) and operation C_o (USD/year) costs during the whole project lifetime L (years) as well nominal interest rate of the alternative investment i (-) related with specific interest value r (-) [8].

The specific interest value r will vary according to the years j during the lifetime L in which the costs are considered. For the specific year it can be generally expressed by Eq. (2):

$$r = (1 + i)^j. \tag{2}$$

The technical criteria for selected battery technologies are presented next.

5.1. Li-ion

Li-ion is a battery technology (electrochemical accumulator) which do not contain pure lithium, but its salts. The assumed type of Li-ion battery is $LiFePO_4$ due to its high overload capability and long lifetime as well as safety. The batteries include a temperature control system that allows short-time overloading by multiples of rated output current without any damage as can be seen in Tab. 2 [9].

The battery rated output current $It = 1$ pu with rated power P (MW) and rated capacity C (MWh). According to [9], the optimal dimensioning of the power to capacity ratio is 1 (i.e., capacity in (MWh) *equals* power (MW)).

Tab. 2: Li-ion overloading example [9].

***It* (pu)**	***P* (MW)**	***C* (MWh)**	**Discharge time** (h)
1	1	1	1
2	2	1	0.5
3	3	1	0.33

There are two main factors which most affect the lifetime of Li-ion battery. They are the Depth of Discharge DoD (%) which is described in Eq. (3) and multiples of the output current It (pu) which is described in Eq. (4) [9]. The standalone aging over time is neglected due to the minor effects.

$$n_1 = 5.6911 \cdot DoD^2 - 1{,}090.3 \cdot DoD + 52{,}119 + x, \tag{3}$$

where n (-) is the number of the working cycles of charge and discharge and x (-) is the nominal number of the working cycles for $DoD = 100$ % and $It = 1$ pu [9].

$$n_2 = 5.6271 \cdot It^2 - 259.45 \cdot It + 253.82 + x. \tag{4}$$

These dependencies lead to the lifetime model of the Li-ion battery which is described in Eq. (5) and presented in Fig. 2 where x was set to 2,500.

$$n = \left(\frac{n_1}{x} \cdot \frac{n_2}{x}\right) \cdot x. \tag{5}$$

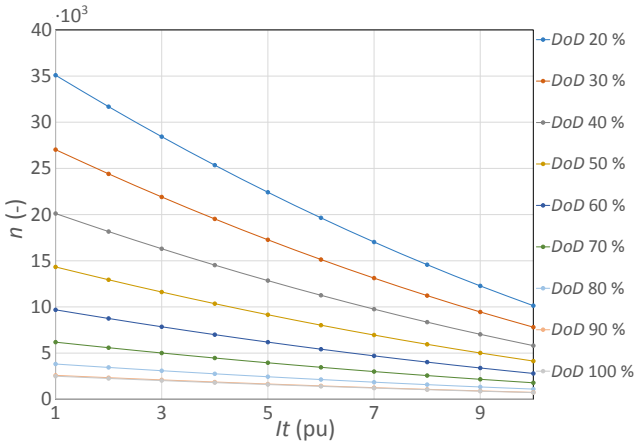

Fig. 2: Lifetime model of the Li-ion battery.

5.2. NaS

NaS is a battery technology that contains molten sodium and sulfur as electrodes and beta alumina as a solid electrolyte. The battery is heated to 300–350 °C in operational state. One of the advantages is the capability to deliver pulse power [10].

The battery rated output current $It = 1$ pu with rated power P (MW) and rated capacity C (MWh). According to the [10], the optimal dimensioning of power to capacity ratio is 6 (i.e., capacity in (MWh) is *six times higher* than the power in (MW)).

NaS batteries can be also overloaded which is shown in Fig. 3 where $t_{\max}$ (h) is the maximal time of the overload [11].

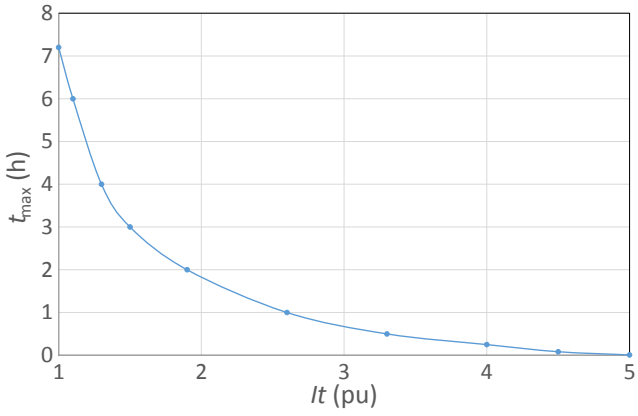

Fig. 3: Overloading capability of the NaS batteries.

Overloading capability can be approximated by Eq. (6) [11]:

$$t_{\max} = 30.425 \cdot e^{-1.395It}. \tag{6}$$

Similarly, to the Li-ion batteries the depth of discharge is affecting a lifetime of NaS too (aging only over time is neglected due to the minor effects). This dependency is described in Eq. (7) where x is set to 4,500 working cycles according to [10]:

$$n = 87{,}495 \cdot DoD^{-0.645} + x. \tag{7}$$

5.3. VRF

VRF battery is one of the most technically applicable flow battery systems. Energy is stored in vanadium redox pairs (V^{2+}/V^{3+} and V^{4+}/V^{5+}) in two electrolyte tanks. The ion exchange takes place through the ion-selective membrane between the tanks as described in [11]. One of the biggest advantages of VRF batteries is their stable capacity during their lifetime. The downside is that they cannot be overloaded, i.e. $It \leq 1$. Due to this fact, the n is equal to x which is set to 12,000 according to the [12]. Also, according to the [12], the optimal dimensioning of power to capacity ratio is 5 (i.e., capacity in (MWh) is *five times higher* than the power in (MW)).

$$n = x. \tag{8}$$

5.4. Results

For the purpose of complex evaluation of the battery technologies based on the presented methodology and equations, a comparison tool which is in detail described in [13], has been developed.

The case study-specific inputs are summarized in Tab. 3, where n_e (-) is the demanded working cycle count.

The capital costs for Li-ion were stated to 400 USD·kWh^{-1} (costs per capacity), NaS to 2,500 USD·kW^{-1} (costs per power) and VRB to 450 USD·kWh^{-1} (cost per capacity), the operation costs were assumed as 2 % of 1 MWh (1 MW for the NaS) [8], [9] and [12].

The outputs are presented in Fig. 4 and summarized in Tab. 4, where n_{real} (-) is the real number of working cycles.

In the comparison focused on future investment and operation costs, it can be clearly seen the benefit of Li-ion technology against NaS and VRB for this application. The advantage is determined primarily by overload capability and associated accurate sizing.

6. Converter Topology

In the design of the BESS, the choice of the topology and a way of coupling to the grid is one of the things that can greatly influence the performance of the whole system. Choice of the topology can improve

Tab. 3: Input parameters.

i (-)	n_e (-)	L (year)	P (MW)	C (MWH)	$t_{\max}$ (h)	$x_{\text{Li-ion}}$ (-)	x_{NaS} (-)	x_{VRB} (-)
0.05	10^4	20	4	1	0.15	2,500	4,500	12,000

Tab. 4: Output parameters.

	n_e (-)	n_{real} (-)	P_{real} (MW)	C_{real} (MWH)	It_{real} (pu)	DoD_{real} (%)	C_f (mil. USD)
Li-ion	10^4	10,021	1.78	1.78	2.24	56.05	2.39
NaS	10^4	14,744	1.05	6.32	1	15.83	8.81
VRB	10^4	12,000	4	20	1	5	30.13

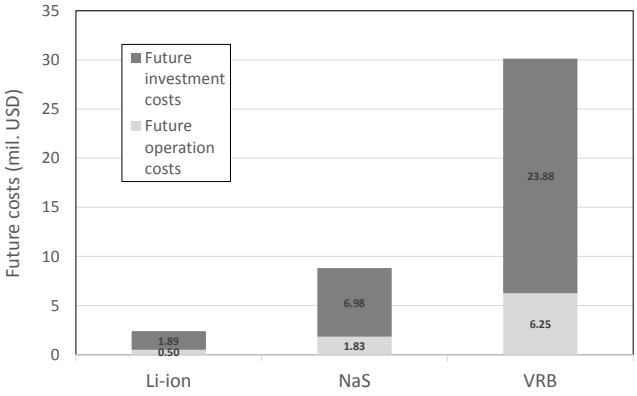

Fig. 4: Battery technology comparison results.

the overall efficiency of the system and reduce possible negative impact on the grid. The choice of the connection to the grid will also influence the way in which the BESS interacts with the grid, both in a good and bad way. The following chapter takes this into account and shows the process, how the final choice of the converter for the BESS has been done.

The second crucial part of the Battery Energy Storage System (BESS) is the power converter, which acts as an interface between the electrical grid and batteries. There are the following basic requirements regarding the converter, influencing chosen converter topology. Firstly, the converter must be bidirectional, because it is not only supplying power to the grid but also charges the batteries.

Another important requirement on the converter is maximal possible energy efficiency and/or minimal losses. Great impact regarding the efficiency of the converter has the choice of the converter voltage. Generally, it can be said that the converter losses, the output filter losses, and transformer losses are proportional to the converter current. A natural way to decrease the current and preserve the power is to increase the voltage. With the present-day semiconductor, it is the use of standard two-level converters very limited in the way of maximal output voltage. For example, with the use of 1.7 kV IGBT transistors, the expected output phase to phase voltage is around 490 V. Hence, it is necessary and, in some respects, even beneficial, to use the multilevel converter topology to reach higher output voltage levels. With the multilevel converter, it is possible to reach voltages up to 10 kV without great complications caused by the insulation distances. Another benefit of the multilevel converter is lower distortion of the output current. This can be used either to lower demands on the output filter or keep the benefit of lesser influence of the convertor switching on the grid.

The first question that needs to be solved is the way of connection of the converter to the grid. There are two main choices serial or shunt type of connection.

6.1. Series Connected Converter

One of the main features of the proposed BESS is the protection of the thermal power plant against transient caused by voltage fluctuation of the grid. From this point of view, the maximal impact for the lowest effort control would have series-connected converters [14].

The first viable technology is the Series Active Filter (SeAF). Conventional SeAF is connected to the grid via a transformer [15]. The transformer is connected in series in the link between the generator and the grid, so it must be able to withstand the full output power of the power plant. There are also transformerless variants of the SeAF [16]. SeAF technology is designed to compensate for voltage disturbance in the grid. This technology is not suitable for use in the BESS. There are complications in the control of the active power flow. Charging and discharging of the batteries could interfere with the generator control.

Better suited for use in the BESS are technologies of Unified Power Flow Controller (UPFC) [17] and [18] and Hybrid Power Flow Controller (HPFC) [19] and [20]. These technologies combine series and shunt active power filters.

Converter technologies mentioned above have common disadvantage, which is one of the components connected in series with the grid. This would greatly raise the cost of the device because there is a great difference between the output power of the power plant and the BESS. Another disadvantage linked to the series component is the intervention in the infrastructure of the power plant during installation of the device and

the last disadvantage is the already mentioned possible interference with the main generator control.

6.2. Shunt Connected Converter

Shunt connected converter is connected in parallel with respect to the other grid sources. This type of converter cannot directly influence the voltage of the grid. It can influence the grid voltage indirectly, using the current supplied to the grid. The great benefit of this technology is absence of the component which needs to withstand power flow through the grid line.

Due to the mentioned reasons shunt connected converter has been chosen as suitable technology. In the next section, the choice of suitable converter topology is discussed.

6.3. Multilevel Topologies

In order, to optimize the topology of the converter, four multilevel converter topologies were analyzed for the BESS application. Suitable multilevel topologies are listed in [21] – topologies based on i) Flying Capacitors (FC), ii) clamping diodes (NPC), iii) Cascaded H-Bridges (CHB) and iv) Modular MultiLevel Converter (MMLC).

The choice of batteries is an important parameter, besides a capacity and an output power, a battery voltage. The battery voltage should be high, to reduce the complexity of the converter. Number of converter levels depends on the output voltage and DC-link voltage. The upper limit of the battery voltage is given by the used transistors. Based on the BESS parameters, suitable transistors have a blocking voltage 1.7 kV and the chosen battery voltage is 881 V [22]. The voltage of this battery ranges from 714 to 1,000 V, depending on the state of charge. Because of the limitations regarding battery voltage, it is beneficial to avoid topologies with the centralized DC-link. This is a case of NPC, FC and MMLC topology with the centralized DC link. It is not impossible to build a battery suitable for these topologies, but because this battery is not commercially available, it would demand additional development of an adequate battery management system or use of an additional DC-DC converter [23]. Then, the remaining topologies are CHB and MMLC with distributed batteries [24]. Finally, the CHB topology was chosen because of the fewer semiconductor components [25].

The Cascaded H-Bridge converter comes out as the best option. In comparison with the competitive topologies, it needs fewer components (clamping diodes or flying capacitors) – i.e., lower investment costs, higher reliability and smaller demands on installation space. Moreover, CHB technology provides an easy way for serial battery connection and a way to balance battery voltages.

There are two CHB topologies, CHB in star connection (CHB-Y) and CHB in delta connection (CHB-D) (see Fig. 5). At first glance, CHB-D topology has the disadvantage of lower output voltage, but it provides a way to balance battery voltage not just in one leg, but it also provides voltage balancing between individual converter legs, using circulating current.

The converter is going to be connected to the grid via output filter and transformer. The rate of turns of the transformer is given by the following conditions. The converter side transformer voltage must be lower than the converter output voltage with enough distance to cope with voltage drop on the output. The maximal output voltage of the converter is given by the voltage of the DC-link. According to this condition, the worst-case scenario is demand of full power combined with discharged battery.

For example, if converter output voltage, calculated for the nominal battery voltage, is 5.7 kV. For the flat battery, the maximal output voltage is 4.5 kV. So, for the choice of the output transformer, maximal depth of discharge has to be taken into account.

Hardware design and control have been simulated in Matlab Simulink and Plecs blockset. Converter and filter design, control design, and simulation results are presented in the following text.

6.4. Converter

The model represents chosen CHB-D converter topology. Used topology respects components available on the market. Based on DC link voltage and desired output voltage, it has been chosen 19 level configuration. That means there are eight H-bridges connected in series in each phase (leg) of the converter.

The model takes into the account switching of the transistors. It shows the influence of the switching frequency and the deadtimes on the control and the output filter.

The design overview of BESS is presented in Fig. 5. The same circuit has been replicated using Plecs blockset. It represents four main parts – the batteries, the converter, the output filter with a transformer and the grid. The grid is modeled as ideal voltage source.

6.5. Filter

The filter is an important part of a grid-connected voltage source converter. It enables the connection of converter step voltage to smooth grid voltage. This is one

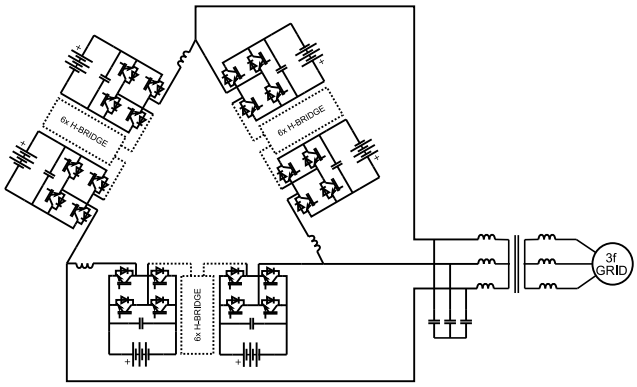

Fig. 5: BESS diagram.

of the parameters considered in the simulation. Simulated waveforms of these voltages are shown in Fig. 6. Connecting a converter without a filter would lead to huge current pulses.

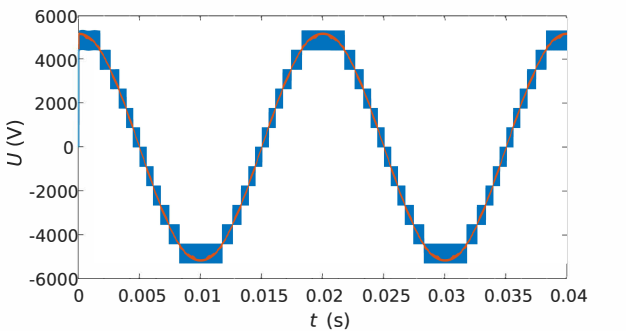

Fig. 6: Converter output voltage (blue), grid voltage (orange).

The simplest kind of output filter is an inductor connected in series between a converter and a grid. This solution is the simplest both from a hardware and control point of view. Its downside is bulkiness, high price, and high voltage drop. A better approach employs LCL filter. In the case of CHB-D converter first inductor is inside the delta connection, because it is not only part of the output filter, but also it helps control the delta connection circulating current. The second inductance is formed by an output transformer leakage inductance.

There is another advantage of a multilevel converter relating to the output filter. Thanks to the higher number of output voltage levels, the output current has a lower ripple in comparison with a standard two-level converter of the same output voltage. This causes lower THD and allows the use of a smaller filter.

6.6. Control

The essential part of the converter is the control which generates control pulses for the power part of the converter. The control complexity of the converter can vary significantly depending on converter abilities and extra features. The basic control, shown in Fig. 8, includes the control of the input/output power and the control of the delta connection current described in Eq. (8). The advanced feature ism, for example, compensation of asymmetries or higher harmonics in a grid.

The base of the control is a Synchronous Reference Frame Phase-Locked Loop (SRF-PLL) [26]. This identifies the voltage of the grid for feedforward control and it provides angle theta of dq rotational frame coordination system. Transformation to the rotational frame is well known in the case of rotational machine control, where it leads to separate control of torque and excitation of the machine [27]. Similar results can be obtained, when used in combination with the grid-tied converter. In this case, it leads to separate control of active and reactive power [28] and [29]. Orientation of the used reference frames is shown in Fig. 7. PLL calculates θ to ensure grid voltage $U_q = 0$. In synchronously rotating reference frame, the following assumption applies – the control of I_d current controls the active power and the control of I_q current controls the reactive power.

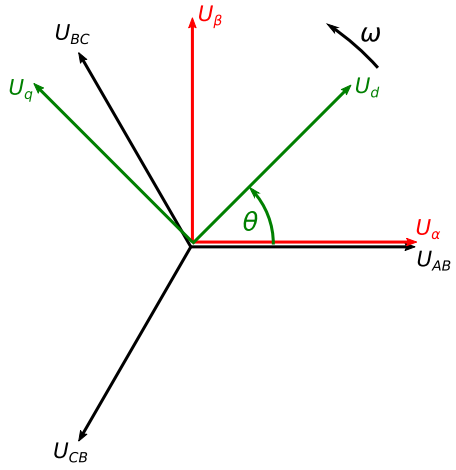

Fig. 7: dq rotational frame coordination system.

Control of the power flow is done by controlling d and q currents. Most of the current control (see Fig. 8) is done by feedforward compensation and PI controllers make slight changes to compensate for errors in the mathematical model used for feedforward.

The feed-forward part of the control algorithms calculates converter output voltage based on grid voltage and voltage drop on the output filter. The voltage drop on the output filter is calculated by its mathematical model and reference of the setpoint power. This leads to a faster response of the storage in case of grid voltage changes or setpoint output power changes.

To get the most stable current control and for the proper function of software protection. The currents

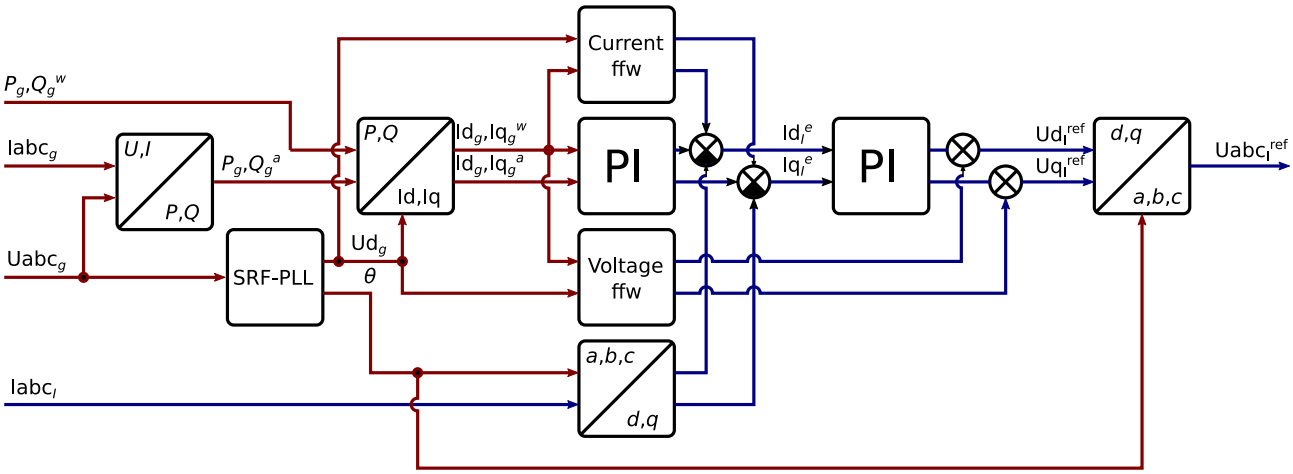

Fig. 8: Diagram of control algorithm.

in individual legs of the converter are used for the current control. This solution has advantages from the converter point of view, but it does not provide precise control of power flow to the grid.

Another part of the control solves the problem stated above, caused by the capacitor of the output filter. Converter should behave neutrally in relation to the grid. But the capacitor of the output filter causes unwanted currents rise of reactive power even in time when the storage should be inactive. To compensate for the difference between power at the output of converter and output of filter the compensation of filter effect on output power is added to the control algorithm. The structure of the power regulation algorithm is shown in Fig. 8. Details including developed feedforward loops will be the subject of a future publication.

Because of the delta connection, a problem with current flowing inside the delta connection can appear. It can be evaluated as the sum of the individual converter phase currents described in Eq. (9). This current can be used for voltage balancing of batteries, but in most cases, this current is unwanted and caused by some parasitic phenomenon, for example, nonlinearity. Trials have shown that the most pronounced component of this current is direct current and third harmonic (150 Hz). The PR controller has been chosen to solve this phenomenon. It addresses discovered issues and can be easily expanded.

$$I_r = \frac{I_{ab} + I_{bc} + I_{ca}}{3}. \tag{9}$$

6.7. Simulation Results

For the testing and tuning purposes, it was simulated a step change of setpoint of the output power from zero to 4 MW. The simulation consists of three parts.

The first part is the start-up of the converter. In the beginning, storage is not connected to the grid and the LCL filter is slowly charged using a voltage ramp – see in Fig. 9. This is preventing an oscillation of the filter.

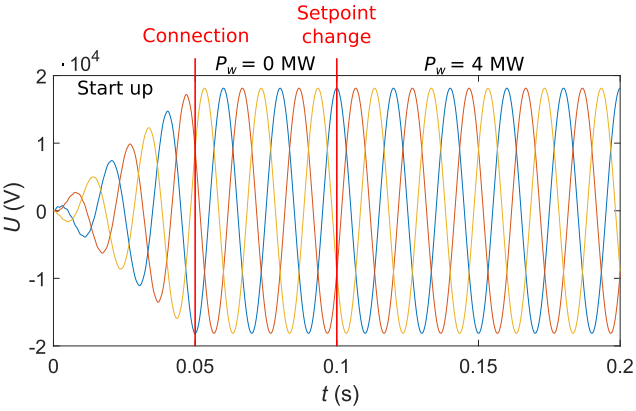

Fig. 9: Output voltage on the grid side of the transformer.

The second part of the simulation starts when the converter is connected to the grid at 0.05 s, a small reactive power is supplied to the grid. This can be observed in Fig. 10 and Fig. 11. This is caused by the capacitors in the output filter. This reactive power is compensated by the control algorithm, at the time of 0.07 s.

The third part starts at the 0.1 s, the setpoint of active output power is changed from zero to 4 MW. The control in the simulation is set for fast response, this leads to small oscillations of the output filter.

The simulation proved, that the control of the converter is stable and can reach the wanted output power in a very short time of 20 ms.

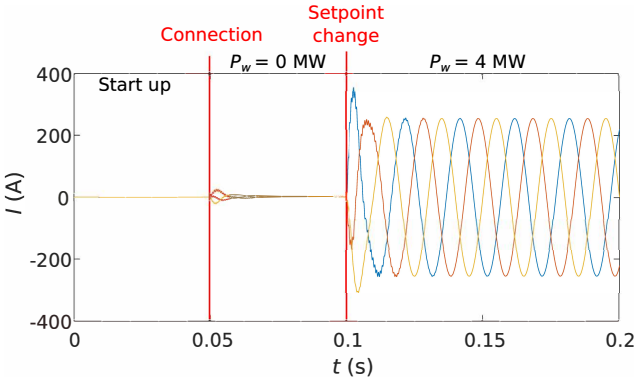

Fig. 10: Output current on the grid side of the transformer.

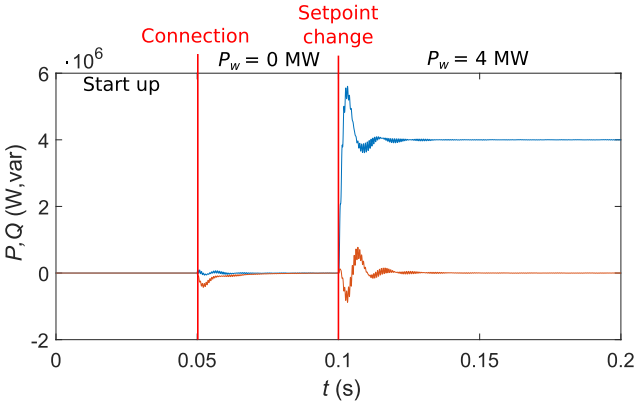

Fig. 11: Output active power (blue), output reactive power (orange).

7. Conclusion

The complex process of energy storage technology and converter topology design suitable for integration in thermal power plant systems was presented in the paper.

Presented methodology has been applied to a real case study based on 200 MW thermal power unit with considered BESS with power 4 MW and capacity 1 MWh.

The general state of the art accumulation technologies has been briefly reviewed and then three battery storage technologies (Li-ion, NaS and VRF) have been evaluated in detail. Li-ion technology has been selected as the most suitable from technical-economical point of view for this type of application.

The next part was focused on a suitable converter topology and control design. Standard multilevel converter topologies were compared (NPC, FC, CHB-Y and CHB-D). A multilevel cascade H-bridge converter design has been selected as the best one. The developed converter control algorithms including simulation verifications were presented as well.

The main converter control parts which control the active and reactive power are complete. The simulation model can be used for control tuning in case of BESS dimensioning change or for the development of advanced control algorithms. Thanks to the fidelity of the storage hardware and topology, it is a useful tool in designing the output filter.

In the future, advanced control features will be added. BESS will be able to serve not just as energy storage, but also as an active filter and symmetrization device. Another converter control upgrade will be an adjustment of the feedforward model to compensate for a reactive power caused by the filter capacitor. This will eliminate the reactive power peak which appeared at the time of connection to the grid (see Fig. 11 - 0.05 s).

Acknowledgment

This work was supported by the Technology Agency of the Czech Republic within the project No. TN01000007 and student research project SGS-2021-021.

Author Contributions

M.V. developed an overview for energy storage technologies, he designed the battery energy storage dimensioning methodology as well as battery comparison methodology. J.D. developed a search for suitable converter topologies, he made a selection of the appropriate topology and designed converter control. M.S. made a corrections of the final version of the manuscript and supervised the whole project.

References

[1] FITIWI, D. Z., S. F. SANTOS, F. P. ANDRE SILVA and P. S. JOAO CATALAO. Impacts of Centralized Energy Storage Systems on Transmission Grid Operation: A Portuguese Case Study. In: *2018 8th International Conference on Power and Energy Systems (ICPES)*. Colombo: IEEE, 2018, pp. 223–228. ISBN 978-1-5386-6029-4. DOI: 10.1109/ICPESYS.2018.8626880.

[2] JOUBERT, C. J., N. CHOKANI and R. S. ABRAHI. Impact of Large Scale Battery Energy Storage on the 2030 Central European Transmission Grid. In: *2018 15th International Conference on the European Energy Market (EEM)*. Lodz: IEEE, 2018, pp. 1–5. ISBN 978-1-5386-1488-4. DOI: 10.1109/EEM.2018.8469789.

[3] MARTINEZ, M., M. G. MOLINA and P. E. MERCADO. Optimal Sizing and Location of Energy Storage System in a Power System. In: *2018 5th International Symposium on Environment-Friendly Energies and Applications (EFEA)*. Rome: IEEE, 2018, pp. 1–6. ISBN 978-1-5386-5517-7. DOI: 10.1109/EFEA.2018.8617103.

[4] OUDALOV, A., D. CHARTOUNI and C. OHLER. Optimizing a Battery Energy Storage System for Primary Frequency Control. *IEEE Transactions on Power Systems*. 2007, vol. 22, iss. 3, pp. 1259–1266. ISSN 1558-0679. DOI: 10.1109/tpwrs.2007.901459.

[5] BRIVIO, C., S. MANDELLI and M. MERLO. Battery energy storage system for primary control reserve and energy arbitrage. *Sustainable Energy, Grids and Networks*. 2016, vol. 6, iss. 1, pp. 152–165. ISSN 2352-4677. DOI: 10.1016/j.segan.2016.03.004.

[6] VINS, M., J. DRAGOUN and M. SIROVY. Integration of Battery Energy Storage in Thermal Power Plant. In: *2020 The 46th Annual Conference of the IEEE Industrial Electronics Society (IECON)*. Singapore: IEEE, 2020, pp. 1608–1613. ISBN 978-1-7281-5414-5. DOI: 10.1109/IECON43393.2020.9254725.

[7] LUO, X., J. WANG, M. DOONER and J. CLARKE. Overview of current development in electrical energy storage technologies and the application potential in power system operation. *Applied Energy*. 2015, vol. 137, iss. 1, pp. 511–536. ISSN 1872-9118. DOI: 10.1016/j.apenergy.2014.09.081.

[8] TSIANIKAS, S., J. ZHOU, D. P. BIRNIE III and D. W. COIT. Economic trends and comparisons for optimizing grid-outage resilient photovoltaic and battery systems. *Applied Energy*. 2019, vol. 256, iss. 1 pp. 1–16. ISSN 1872-9118. DOI: 10.1016/j.apenergy.2019.113892.

[9] OMAR, N., M. A. MONEM, Y. FIROUZ, J. SALMINEN, J. SMEKENS, O. HEGAZY, H. GAULOUS, G. MULDER, P. VAN DEN BOSSCHE, T. COOSEMANS and J. VAN MIERLO. Lithium iron phosphate based battery – Assessment of the aging parameters and development of cycle life model. *Applied Energy*. 2014, vol. 113, iss. 1, pp. 1575–1585. ISSN 1872-9118. DOI: 10.1016/j.apenergy.2013.09.003.

[10] Products: NAS Batteries. In: *NGK INSULATORS, LTD* [online]. 2020-2-20. Available at: https://www.ngk.co.jp/nas/specs.

[11] SARASUA, A. E., M. G. MOLINA and P. E. MERCADO. *Energy Storage - Technologies and Applications: Dynamic Modelling of Advanced Battery Energy Storage System for Grid-Tied AC Microgrid Applications*. 1st ed. London: IntechOpen Limited, 2013. ISBN 978-953-51-6296-4.

[12] Vanadium Redox Flow Machines. In: *RedT Energy: Industrial Energy Storage Solutions* [online]. 2020-2-16. Available at: `https://www.redtenergy.com/solutions/vanadium_redox_flow_machines`.

[13] VINS, M. and M. SIROVY. Assessing Suitability of Various Battery Technologies for Energy Storages : Lithium-ion, Sodium-sulfur and Vanadium Redox Flow Batteries. In: *2020 International Conference on Applied Electronics (AE)*. Pilsen: IEEE, 2020, pp. 1–5. ISBN 978-80-261-0892-4. DOI: 10.23919/AE49394.2020.9232919.

[14] JAVADI, A., N. GEISS, H. F. BLANCHETTE and K. AL-HADDAD. Series active conditionners for reliable Smart grid: A comprehensive review. In: *IECON 2012 - 38th Annual Conference on IEEE Industrial Electronics Society*. Montreal: IEEE, 2012, pp. 6320–6327. ISBN 978-1-4673-2421-2. DOI: 10.1109/IECON.2012.6389016.

[15] HUA, C.-C. and C.-W. CHUANG. Design and Implementation of a Hybrid Series Active Power Filter. In: *2005 International Conference on Power Electronics and Drives Systems*. Kuala Lumpur: IEEE, 2005, pp. 1322–1326. ISBN 0-7803-9296-5. DOI: 10.1109/PEDS.2005.1619892.

[16] PINTO, J. G., H. CARNEIRO, B. EXPOSTO, C. COUTO and J. L. AFONSO. Transformerless series active power filter to compensate voltage disturbances. In: *Proceedings of the 2011 14th European Conference on Power Electronics and Applications*. Birmingham: IEEE, 2011, pp. 1–6. ISBN 978-90-75815-14-6.

[17] KANO, M., T. MAEKAWA, T. TAKESHITA and Y. KUNII. Comparison of converter arrangement of series and shunt converters in UPFC for distribution system control. In: *2016 IEEE International Conference on Renewable Energy Research and Applications (ICRERA)*. Birmingham: IEEE, 2016, pp. 431–436. ISBN 978-1-5090-3388-1. DOI: 10.1109/ICRERA.2016.7884374.

[18] BALAKRISHNAN, F. G., S. K. SREEDHARAN and J. MICHAEL. Transient stability improvement in power system using unified power flow controller (UPFC). In: *2013 Fourth International Conference on Computing, Communications and*

Networking Technologies (ICCCNT). Tiruchengode: IEEE, 2013, pp. 1–6. ISBN 978-1-4799-3926-8. DOI: 10.1109/ICCCNT.2013.6726841.

[19] SHOTORBANI, A. M., X. MENG, L. WANG and B. MOHAMMADI-IVATLOO. A Decentralized Multiloop Scheme for Robust Control of a Power Flow Controller With Two Shunt Modular Multilevel Converters. *IEEE Transactions on Industrial Informatics*. 2018, vol. 14, iss. 10, pp. 4309–4321. ISSN 1941-0050. DOI: 10.1109/TII.2018.2799139.

[20] MERRITT, N. R. and D. CHATTERJEE. Performance improvement of power systems using Hybrid Power Flow Controller. In: *2011 International Conference on Power and Energy Systems*. Chennai: IEEE, 2011, pp. 1–6. ISBN 978-1-4577-1510-5. DOI: 10.1109/ICPES.2011.6156628.

[21] SOONG, T. and P. W. LEHN. Evaluation of Emerging Modular Multilevel Converters for BESS Applications. *IEEE Transactions on Power Delivery*. 2014, vol. 29, iss. 5, pp. 2086–2094. ISSN 1937-4208. DOI: 10.1109/TPWRD.2014.2341181.

[22] Advanced batteries for energy storage. In: *LG Chem* [online]. 2018. Available at: `https://www.lgchem.com/upload/file/product/LGChem_Catalog_Global_2018.pdf`

[23] SHI, Y., R. LI and H. LI. Modular multilevel dual active bridge DC-DC converter with ZVS and fast DC fault recovery for battery energy storage systems. In: *2016 IEEE Applied Power Electronics Conference and Exposition (APEC)*. Long Beach: IEEE, 2016, pp. 1675–1681. ISBN 978-1-4673-9550-2. DOI: 10.1109/APEC.2016.7468092.

[24] VASILADIOTIS, M. and A. RUFER. Analysis and Control of Modular Multilevel Converters With Integrated Battery Energy Storage. *IEEE Transactions on Power Electronics*. 2015, vol. 30, iss. 1, pp. 163–175. ISSN 1941-0107. DOI: 10.1109/TPEL.2014.2303297.

[25] BARUSCHKA, L. and A. MERTENS. Comparison of Cascaded H-Bridge and Modular Multilevel Converters for BESS application. In: *2011 IEEE Energy Conversion Congress and Exposition*. Phoenix: IEEE, 2011, pp. 909–916. ISBN 978-1-4577-0541-0. DOI: 10.1109/ECCE.2011.6063868.

[26] MERAL, M. E. and D. CELIK. DSOGI-PLL Based Power Control Method to Mitigate Control Errors Under Disturbances of Grid Connected Hybrid Renewable Power Systems. *Advances in Electrical and Electronic Engineering*. 2018, vol. 16, iss. 1, pp. 81–91. ISSN 1804-3119. DOI: 10.15598/aeee.v16i1.2485.

[27] HU, T. and X. ZHANG. Simulation of PMSM Vector Control System Based on Fuzzy PI Controller. In: *2019 IEEE International Conference on Power, Intelligent Computing and Systems (ICPICS)*. Shenyang: IEEE, 2019, pp. 111–114. ISBN 978-1-7281-3720-9. DOI: 10.1109/ICPICS47731.2019.8942439.

[28] CROWHURST, B., E. F. EL-SAADANY, L. EL CHAAR and L. A. LAMONT. Single-phase grid-tie inverter control using DQ transform for active and reactive load power compensation. In: *2010 IEEE International Conference on Power and Energy*. Kuala Lumpur: IEEE, 2010, pp. 489–494. ISBN 978-1-4244-8946-6. DOI: 10.1109/PECON.2010.5697632.

[29] GAO, Y. and J. YE. A SVPWM Compensation Current Tracking Control Method Based on dq Transformation for Shunt Active Power Filter. In: *2018 International Conference on Virtual Reality and Intelligent Systems (ICVRIS)*. Hunan: IEEE, 2018, pp. 433–436. ISBN 978-1-5386-8031-5. DOI: 10.1109/ICVRIS.2018.00112.

About Authors

Martin VINS received his master's degree in 2018 in the University of West Bohemia (UWB) at the Faculty of Electrical Engineering, Pilsen, Czech Republic. In the same year, he started Ph.D. study and has joined the Regional Innovation Centre for Electrical Engineering (RICE) at UWB.

Jaroslav DRAGOUN received his master's degree in 2018 in the University of West Bohemia (UWB) at the Faculty of Electrical Engineering, Pilsen, Czech Republic. In the same year, he started Ph.D. study and has joined the Regional Innovation Centre for Electrical Engineering (RICE) at UWB.

Martin SIROVY received his Ph.D. degree in 2014 from the University of West Bohemia (UWB) at the Faculty of Electrical Engineering, Pilsen, Czech Republic. In 2010, he has joined the Regional Innovation Centre for Electrical Engineering (RICE) at UWB, since 2018 he has been a head of Complex System Solutions Department.